Genomic and physiological characterization of the chromate-reducing, aquifer-derived firmicute *Pelosinus* sp. strain HCF1

Harry R. Beller*, Ruyang Han, Ulas Karaoz, HsiaoChien Lim, Eoin L. Brodie

Earth Sciences Division, Lawrence Berkeley National Laboratory, Berkeley, CA 94720

Running title: Genome and physiology of *Pelosinus* sp. strain HCF1

***Corresponding author:**

Harry R. Beller
Lawrence Berkeley National Laboratory
1 Cyclotron Rd., MS 70A-3317
Berkeley, CA 94720

E-mail HRBeller@lbl.gov
Phone (510) 486-7321
Fax (510) 486-5686

Abstract

Pelosinus spp. are fermentative firmicutes that were recently reported to be prominent members of microbial communities at contaminated subsurface sites in multiple locations. Here we report metabolic characteristics and their putative genetic basis in *Pelosinus* sp. strain HCF1, an isolate that predominated anaerobic, Cr(VI)-reducing columns constructed with aquifer sediment. Strain HCF1 ferments lactate to propionate and acetate (the methylmalonyl-CoA pathway was identified in the genome) and its genome encodes two [NiFe]- and four [FeFe]-hydrogenases for H_2 cycling. Reduction of Cr(VI) and Fe(III) may be catalyzed by a flavoprotein with 42-51% sequence identity to both ChrR and FerB. This bacterium has unexpected capabilities and gene content associated with reduction of nitrogen oxides, including dissimilatory reduction of nitrate to ammonium (two copies of NrfH and NrfA were identified along with NarGHI) and a nitric oxide reductase (NorCB). In this strain, either H_2 or lactate can act as a sole electron donor for nitrate, Cr(VI), and Fe(III) reduction. Transcriptional studies demonstrated differential expression of hydrogenases and nitrate and nitrite reductases. Overall, the unexpected metabolic capabilities and gene content reported here broaden our perspective on what biogeochemical and ecological roles this species might play as a prominent member of microbial communities in subsurface environments.

Introduction

The throughput, depth, and reduced cost of second-generation DNA sequencing facilitates our ability to gain insight into a broad range of microbiological processes in the environment, and genome sequencing of prominent members of environmental microbial communities should contribute to the understanding of complex biogeochemical systems. Members of the *Veillonellaceae*, and particularly *Pelosinus* spp., have recently been reported to

be among the more abundant bacterial taxa in chromate-reducing systems inoculated with material from the chromium-contaminated aquifer at the U.S. Department of Energy (DOE) Hanford 100H site in Washington state (1, 2) and in other contaminated aquifers (3-5). Chromate-reducing bacteria are of interest because *in situ* reductive immobilization is favored as one of the more cost-effective approaches to remediation of aquifers contaminated with Cr(VI), a potent toxicant, mutagen, and carcinogen (6, 7). Fermentative bacteria such as *Pelosinus* spp. may be of particular relevance to a common bioremediation scenario in which metabolism of organic electron donors (e.g., lactate-based polymers) injected into the subsurface readily consume available electron acceptors (e.g., oxygen, nitrate, sulfate, ferric iron) and drive the treated zone towards fermentative/methanogenic conditions.

In this article, we report on a variety of metabolic capabilities and their possible underlying genetic basis in a *Pelosinus* isolate that dominated a chromate-reducing community derived from aquifer sediment from the Hanford 100H site. The metabolic capabilities explored include lactate fermentation to propionate and acetate (related to the methylmalonyl-CoA pathway identified in the genome), Cr(VI) and Fe(III) reduction (both potentially related to identified flavoproteins), nitrate and nitrite reduction (potentially related to NrfH and NrfA, as well as a membrane-bound, respiratory nitrate reductase), and H_2 metabolism (two [Ni-Fe]-hydrogenases and four [FeFe]-hydrogenases were identified). We also report on focused transcriptional studies designed to more clearly associate certain genes with specific metabolic activities (namely, H_2 cycling and nitrate or nitrite reduction). Some metabolic activities and gene content reported here are unexpected for *Pelosinus* species and broaden our perspective on what metabolic and ecological roles this species might play in microbial communities in contaminated (and uncontaminated) environments.

MATERIALS AND METHODS

Isolation and cultivation of *Pelosinus* sp. strain HCF1. *Pelosinus* sp. strain HCF1 was isolated from the effluent of an anaerobic, chromate-reducing, flow-through column containing aquifer sediment from the DOE Hanford 100H site and eluted with sterile, synthetic groundwater. The synthetic groundwater contained the following constituents: 1 mM phosphate buffer (0.58 mM K_2HPO_4 and 0.42 mM KH_2PO_4; pH 7), 1.25 mM $NaHCO_3$, 0.25 mM $CaCl_2$, 0.1 mM NH_4Cl, 5 mM sodium lactate (the carbon source and electron donor), 5 μM $KCrO_4$, and 7.5 mM Na_2SO_4. Highly purified water (18 MΩ resistance) obtained from a Milli-Q Biocel system (Millipore, Bedford, MA) was used to prepare the synthetic groundwater and all other aqueous solutions described in this article. Although sulfate was available as an electron acceptor, ion chromatographic monitoring of the effluent confirmed that lactate was fermented to acetate and propionate and that sulfate reduction was not required for this process.

Isolation of strain HCF1 from column effluent was accomplished using a modified Hungate roll-tube technique (8) with serial dilutions to 10^{-5}. Direct microscopic cell counts showed that there were approximately $1x10^7$ cells/mL in the effluent samples. Basal medium (0.58 mM K_2HPO_4, 0.42 mM KH_2PO_4, 0.25 mM $CaCl_2$, 0.1 mM NH_4Cl) containing 2% Noble agar and amended with 20 mM sodium lactate, 10 mM $NaHCO_3$, and vitamin, trace element, and selenite-tungstate solutions described elsewhere (9) was used for isolation. The inoculated roll tubes were incubated at 30°C for 7-10 days until bacterial colonies appeared. Second and third rounds of purification were conducted until the cells and colonies were uniform based on microscopic examination. Although yeast extract is not essential for the growth of strain HCF1, 0.5 g/L yeast extract was routinely used in the medium to facilitate growth and colony formation.

After isolation, routine cultivation of strain HCF1 was carried out under strictly anaerobic conditions in an anaerobic glove box (Coy Laboratory Products, Inc., Grass Lake, Mich.) with a nominal gas composition of 86% N_2 – 10% CO_2 – 4% H_2. The growth medium was the same as the medium used for isolation with the omission of Noble agar. Anaerobic techniques used in the preparation of growth medium and stock solutions are described elsewhere (10).

Cell suspension experiments testing Cr(VI) and Fe(III) reduction by strain HCF1. All cell suspension experiments described in this article were performed under strictly anaerobic conditions in an anaerobic glove box. The glass and plastic materials used to contain or manipulate the cultures were allowed to degas in the glove box for at least one day before use. Cell suspension assays performed to assess chromate reduction by strain HCF1 under fermentative conditions were conducted in a similar manner to those described previously for *Pseudomonas* sp. strain RCH2 (9). Strain HCF1 was grown anaerobically at 30°C in a glove box, harvested in mid log phase (OD ≈ 0.2, after 48 hr of incubation) by anaerobic centrifugation (11,899 x g, 15 min, 15 °C), washed with 100 mL anaerobic basal medium, and resuspended anaerobically in the glove box. Assays were performed in butyl rubber-stoppered Balch tubes and initiated by adding 1 mL of concentrated cells to 9 mL of basal medium amended with the appropriate compounds, such as 50 μM chromate and 20 mM lactate (final concentration). Assays were run in duplicate at ~30°C. Samples (500 μL) were collected before cells were added, immediately after cell addition, and typically every 30 min thereafter. 200 μL of the suspension was used for OD_{600} (optical density at 600 nm) measurement and the remainder was spun down at ~20,800 x *g* (4°C, 4 min). The freshly prepared supernatants and cell pellets were used for various analyses described below. Controls included assays that did not contain lactate (normally added at 20 mM) and in which cells were inactivated by heating (under anaerobic

conditions) in a boiling water bath for 15 min. The potential role of extracellular reductants in Cr(VI) reduction was investigated by conducting assays in 10 mL of filtered (0.2-μm pore size) spent medium after growth or 10 mL of filtered, spent medium that had been heat-denatured anaerobically in a boiling water bath for 15 min. These tests of extracellular reductants were initiated by adding 50 μM $KCrO_4$.

Anaerobic cell suspension experiments to assess reduction of Fe(III) (2 mM) under fermentative conditions were conducted as described for Cr(VI) reduction studies, except that un-centrifuged samples (not supernatants) were used for determination of the reduced metal. Fe(III)-NTA stock solutions (100 mM) were prepared by dissolving 0.82 g $NaHCO_3$, 1.28 g of trisodium nitrilotriacetic acid (Na_3NTA), and 1.35 g of $FeCl_3 \bullet 6H_20$ in 50 mL anaerobic H_2O in an anaerobic glove box and filter-sterilizing into an anaerobic serum bottle. Amorphous $Fe(OH)_3$ was prepared as described previously (11) and stored in an anaerobic glove box for at least several weeks before use to de-oxygenate.

Analytical methods. Analytical methods for all analytes other than Fe(II) were described in detail previously (9) and are briefly summarized here. For routine determination of cell density, OD_{600} of diluted samples was measured using a Model UV160U spectrophotometer (Shimadzu Corporation). It was determined that 1 OD_{600} unit was equivalent to $1x10^9$ cells/mL. Direct microscopic cell counts were also determined in cell suspension experiments. Lactate, acetate, propionate, nitrate, and nitrite concentrations were measured by ion chromatography (IC) using a Model ICS-2000 IC (Dionex Corporation) (9). Cr(VI) in cell suspension supernatants was determined with a spectrophotometric DPC (diphenylcarbazide) microplate assay (9). Total Cr in cell suspension supernatants was measured by inductively coupled plasma-mass spectrometry (ICP-MS) (9).

Fe(II) generated from Fe(III)-NTA or $Fe(OH)_3$ reduction by HCF1 cells was measured with a spectrophotometric Ferrozine assay conducted in an anaerobic glove box. The microplate assay used in this study was adapted from a method described by Stookey (12). Microplates (96-well) that had been stored in an anaerobic glove box for at least one day were amended with 90 µL of 1N HCl, and a 10 µL cell suspension sample was added to the HCl immediately after sampling. Then, 100 µL of Ferrozine solution (1 g/L Ferrozine, 500 g/L ammonium acetate) was added to the acidified sample. After a 10-min incubation, absorbance at 555 nm was measured using a Model 550 microplate reader (Bio-Rad). Fe(II) standards (0.2, 0.5, 1, and 2 mM ferrous ammonium sulfate hexahydrate in 1N HCl) were included on each microtiter plate.

Phylogenetic analysis of microbial communities in Hanford flow-through columns. DNA was extracted from effluent of the same fermenting columns from which strain HCF1 was originally isolated. Effluents were collected directly into 50-mL tubes containing 30 ml of an RNA preservation reagent (25 mM sodium citrate, 10 mM EDTA, 10 M ammonium sulfate, pH 5.2). After overnight incubation at 4 ºC, the solution was filtered (0.22-µm pore size) and DNA and RNA co-extracted from filter sections using a modification of the extraction procedure reported by Ivanov and co-workers (13). This modification involved the addition of 1 g of Chelex-100 to the extractions to chelate iron; all other procedures were as reported.

Extracted DNA (10 ng) was used as a template for PCR amplifications using primers (515F and 907R) targeting the V4-V5 hypervariable regions of the SSU rRNA gene with error-correcting barcodes (14):

515F-454:

5’ CCTATCCCCTGTGTGCCTTGGCAGTCTCAG<u>AG</u>**GTGCCAGCMGCCGCGGTAA** ’3

907R-454:

5’CCATCTCATCCCTGCGTGTCTCCGACTCAG*GTGAGGTCGCTA*<u>AC</u>**CCGTCAATTCCT**

TTRAGTTT ‘3

where underlined text represents a spacer, italics represents a barcode, and bold text represents a priming region.

PCR reactions were performed using Takara Ex Taq polymerase, 0.625 units (Takara, Madison, WI), 1X reaction buffer, 200 μM dNTPs, 0.56 mg/mL BSA, and 1 μM each primer with the following thermocycling parameters: initial denaturation at 95 °C for 1 min followed by 25 cycles of 95 °C for 20 sec, 30 sec of annealing at 66 °C and extension at 72 °C for 1 min. Final product extension was at 72 °C for 10 min. Reaction primer dimers were removed from the PCR products via SPRI bead purification according to the manufacturer’s protocol (AMPure XP, Beckman Coulter Genomics, Danvers, MA) before being checked for quality and quantity on a Bioanalyzer 2100 using a DNA 7500 chip (Agilent Technologies, Santa Clara, CA). Each PCR sample was normalized to 30 ng and samples were combined for multiplex sequencing. Sequencing libraries were created using the LV emu-PCR kit (Lib-L, Roche, Indianapolis, IN) and sequencing conducted on a GS-FLX sequencer (Roche, Indianapolis, IN) at the Veterans Medical Research Foundation, La Jolla, CA.

Analysis of pyrotag sequences was performed using the QIIME suite of tools (15), including quality filtering to Q20, clustering at 97% sequence homology and classification using the RDP classifier (16).

Phylogenetic analysis of strain HCF1. The 16S rRNA gene of strain HCF1 was amplified by the PCR using a universal bacterial 16S forward primer 27F (5’-AGAGTTTGATCCTGGCTCAG-3’) and reverse primer 1492R (5’-TACCTTGTTACGACTT-3’) (17). PCR products were cloned using One Shot TOP10 Chemically Competent *E. coli* and a

TOPO TA Cloning Kit (Invitrogen) and were sequenced at the UC Berkeley DNA Sequencing Facility (Berkeley, CA). The 16S rRNA gene sequence of strain HCF1 was BLASTed (18) against the GenBank nr and RDPII databases. A 16S rRNA phylogenetic tree was generated using MEGA version 4 (19).

Genome sequencing, assembly, and annotation. Genomic DNA library construction for Illumina sequencing of strain HCF1 was performed using the Nextera DNA Sample Prep Kit (Illumina Compatible) according to the manufacturer's instructions using the LMW buffer (Epicenter Biotechnologies, WI). Fragment size distribution estimated using an Agilent Bioanalyzer (Agilent, CA) was centered at 400 bp with a distribution between 200-700 bp. The genome sequencing was performed on the Illumina platform (GAIIx) using a paired-end read library of read length 100 bp with an insert size of 450 bp. We obtained a total of 4,183,216 pairs of reads, corresponding to an estimated 40- to 80-fold coverage of the genome assuming a genome size of 5 to 10 Mb. All raw reads were quality-trimmed to an error probability of 1 in 1000 (Q30). After trimming, reads shorter than 20 nucleotides were removed. 3,957,260 reads were assembled *de novo* using Velvet (20) (k = 57, coverage cutoff = 24, expected coverage = 48, insert size = 450), generating 214 contigs with a N50 length of 79.5 kb.

Genome annotation was first performed automatically using the JGI IMG portal (21) and then manually curated (as described in the Results and Discussion). A search for the CXXCH heme-binding motif that characterizes *c*-type cytochromes was carried out using JGI IMG and ScanProSite (http://prosite.expasy.org/scanprosite/) search tools.

Transcriptional (RT-qPCR) analysis of nitrate and nitrite reduction by strain HCF1

DNA/RNA extraction. Duplicate 50-mL cultures of HCF1 were grown anaerobically using routine medium supplemented with 20 mM lactate with or without 5 mM NaNO3. Five-mL

samples of HCF1 cultures were collected in triplicate after 36 hours and 72 hours and immediately mixed with two volumes of the RNA preservation reagent described previously. Cells were then harvested anaerobically by centrifugation (10,300 x *g*, 20 min, 4°C) and DNA and RNA were extracted using an AllPrep DNA/RNA mini Kit (QIAGEN Sciences, Inc.). Cell pellets were resuspended in 600 µL RLT Plus buffer containing 1% β-mercaptoethanol and homogenized using a FastPrep-24 homogenization system (MP Biomedicals). DNA/RNA samples were then extracted according to the manufacturer's instructions except that the residual DNA in RNA samples was digested on-column using RNase-Free DNase (QIAGEN) for 15 min. DNA/RNA samples were finally eluted in 30 µl RNase-free water and quantified using a NanoDrop 1000 Spectrophotometer (Thermo Fisher Scientific Inc.). DNA/RNA samples were stored at -80°C.

PCR amplification. For calibration standards, gene-specific primers were designed to amplify the *rpoB*, *narG*, *nrfH1*, and *nrfH2* genes from strain HCF1 (Table S1). PCR primers were designed with Primer 3 software (22). Fifty-µL PCR mixtures contained: 5 µL of 5X Ex Taq Buffer; 4 µL of dNTP Mix (2.5 mM of each dNTP); 2.5 µM forward and reverse primer (2 µL each); 0.3 µL TaKaRa Ex Taq DNA polymerase (Takara Bio Inc.); 100 ng DNA template, and nuclease-free water. PCR amplification was performed using a BioRad iCycler (Bio-Rad Laboratories) and the following thermocycling program: 2 min at 98°C; 30 cycles of 10 sec at 98°C, 30 sec at 55°C, 2 min at 72°C; 7 min at 72°C; maintained at 4°C. PCR products were purified using a QIAquick PCR purification Kit (QIAGEN). Amplicons of the *rpoB*, *narG*, *nrfH1,* and *nrfH2* genes were purified, quantified (NanoDrop 1000 spectrophotometer), and serially diluted as DNA templates for calibration (10 to 10^5 copies/reaction).

RT-qPCR analysis. qPCR primers were designed with Primer 3 software. For each RNA sample, cDNA products were synthesized by SuperScript III reverse transcriptase and random hexamers (Invitrogen Corporation) according to the manufacturer's instructions except that 2 µL 10 mM dNTP and 1 µL SuperaseIn (Ambion) were used in each RT reaction to inhibit RNA degradation. Eleven µL RNA was used as template in each 20-µL RT reaction. After RT, 20 µL final cDNA was ten-fold diluted by adding 180 µL nuclease-free water. For qPCR, 20-µL qPCR reaction mixtures contained 10 µL 2X SYBR Green Supermix (Bio-Rad Laboratories), 2.5 µM forward and reverse primers (Table S1) (2 µL each), diluted cDNA template (5 µL), and 1 µL nuclease-free water. qPCR analysis was performed with a MyiQ Single-Color Real-Time PCR Detection System (Bio-Rad Laboratories) using the following temperature cycling program: 2 min at 50°C; 8.5 min at 95°C; 40 cycles of 15 sec at 95°C, 30 sec at 50°C, 30 sec at 70°C, and 15 sec at 81°C. The real-time data were acquired at the 81°C-stage to exclude noise from primer dimers. For each gene, 5-point standards containing 10, 10^2, 10^3, 10^4, and 10^5 copies/reaction were included in the same qPCR run to generate the calibration curve for absolute quantification.

Transcriptional (RT-qPCR) analysis of hydrogenases in strain HCF1

DNA/RNA extraction. One hundred-mL cultures of HCF1 were grown anaerobically using routine medium supplemented with 20 mM lactate or 20 mM fructose. Anaerobically, cells were then spun down, washed, resuspended in 10 mL basal medium supplemented with the same substrates (20 mM lactate or 20 mM fructose), 10 mM $NaHCO_3$, and fixed with a headspace of 80% N_2 / 20% CO_2. In addition, 100 mL of lactate-grown HCF1 cells were resuspended in 10 mL basal medium with 10 mM $NaHCO_3$, and fixed with a headspace of 90% H_2 / 10% CO_2. After 1 hr of incubation, triplicate 3-mL samples (~3 x 10^9 cells) were mixed with 6 mL of the RNA preservation reagent described previously prior to RNA isolation.

PCR amplification and RT-qPCR analysis. PCR amplification to make calibration standards and RT-qPCR conditions were the same as described previously, except that PCR and qPCR primers for the six target hydrogenase genes from strain HCF1 are given in Table S2.

Nucleotide sequence accession numbers. Draft genome sequence data for *Pelosinus* sp. strain HCF1 have been deposited in GenBank under accession number [XX-*will be added in proofs*-XX]. 16S rRNA gene pyrotag sequence data for the flow-through column from which strain HCF1 was isolated have been deposited in the MG-RAST database under accession number 4502869.3.

RESULTS AND DISCUSSION

Lactate fermentation to propionate and acetate. *Pelosinus* sp. strain HCF1 ferments a range of sugars and short-chain mono-and dicarboxylic acids to propionate and acetate. For example, lactate, which has been used in polymeric form (glycerol polylactate) to stimulate *in situ* reductive immobilization of chromium in groundwater (23), is fermented to propionate and acetate in a 2:1 ratio (Figure S1). In addition to lactate, carboxylic acids and sugars that serve as growth substrates and are fermented to propionate and acetate include the following (propionate:acetate ratios are in parenthesis): fumarate (1.5:1), fructose (2:1), glucose (2:1), cellobiose (2:1), and mannitol (4:1). These ratios were determined during growth in the absence of yeast extract or H_2 in the initial headspace.

Chromate reduction by strain HCF1 under fermentative conditions. Anaerobic suspensions of lactate-grown cells of strain HCF1 reduced chromate in a minimal, anaerobic buffer containing 20 mM lactate as the electron donor and no electron acceptor (other than ~45 μM chromate)(Figure 1A). The initial, specific rate of Cr(VI) reduction was ~1.5 x 10^{-11} μmol hr^{-1} $cell^{-1}$. Chromate reduction was much slower in the absence of lactate than in its presence, and

was negligible in controls with killed cells and lactate (Figure 1A). Whereas Figure 1A depicts dissolved Cr(VI) concentrations based on the DPC assay, which is specific to Cr(VI), Figure 1B depicts total dissolved Cr concentrations as determined by ICP-MS. Comparison of the results shown in Figures 1A and 1B, which are based on aliquots from the same samples, makes it clear that strain HCF1 reduced Cr(VI) but that the reduced Cr did not precipitate, even though Cr(III) would be expected to form poorly soluble oxides or hydroxides at pH values > 5 (24). The bacterial production of reduced, soluble Cr has been observed previously, for example in *Pseudomonas stutzeri* strain RCH2 (9), and may be attributable to formation of Cr(III)-organic complexes [e.g., Cr(III)-NAD^+ complexes formed during Cr(VI) reduction by flavin reductases; (25, 26)] or to kinetic limitations on Cr(III) precipitation. Notably, the Cr(VI) and total Cr concentration profiles for the no-lactate control were similar to each other (Figure 1), suggesting that the small amount of Cr(VI) reduced under these conditions precipitated. It is not clear why reduced Cr precipitated more readily in the cell suspensions without lactate, but it is possible that a soluble Cr(III)-propionate complex formed in lactate-containing cultures. In the absence of lactate, the electron donor may have been hydrogen, which is typically present in the glove box atmosphere at 1 to 2%. Additional experiments suggested that H_2 could serve as an electron donor for Cr(VI) reduction, albeit not a very favorable one (Figure S2). Experiments were also conducted to test the possibility that soluble chemical reductants or redox-active proteins were released by strain HCF1 during metabolism of lactate that might cause extracellular Cr(VI) reduction. These cell-free experiments used filtrates of spent medium after growth of strain HCF1 with lactate; the filtrates were tested with and without heat denaturation under anaerobic conditions. In all cases, no Cr(VI) reduction was detected (data not shown), ruling out the role of extracellular chromate reduction by biogenic chemical reductants. These experiments did not

address the possibility of chromate-inducible extracellular enzymes, because the filtrates derived from cells grown in the absence of chromate.

Anaerobic Fe(III) reduction by strain HCF1. Although strain HCF1 is primarily characterized by its fermentative metabolism, it is capable of anaerobic Fe(III) reduction under the tested growth conditions (data not shown) and in cell suspensions. Anaerobic suspensions of lactate-grown cells of strain HCF1 reduced soluble Fe(III) in a minimal, anaerobic buffer containing 20 mM lactate as the electron donor and Fe(III)-NTA as the electron acceptor (Figure 2). In the absence of cells or when cells were anaerobically autoclaved before resuspension, Fe(III) reduction was negligible (Figure 2). Analogous to observations for Cr(VI) reduction studies, a small amount of Fe(III) was reduced when cells were suspended in the absence of lactate. Presumably, reducing equivalents were supplied by H_2 in the glove box atmosphere, as suggested by cell suspension studies in which H_2 was supplied as the sole electron donor at a range of concentrations (Figure S3). Clearly, H_2 is a more effective electron donor for Fe(III) reduction than Cr(VI) reduction (Figures S2 and S3). The specific rate of Fe(III) reduction in the presence of lactate was ~1.5 x 10^{-9} μmol hr^{-1} $cell^{-1}$ [approximately 100-fold faster than the rate of Cr(VI) reduction]. When solid-phase Fe(III), such as synthetic, amorphous $Fe(OH)_3$, was used rather than Fe(III)-NTA, the Fe(III) reduction rate was orders of magnitude slower (data not shown).

Anaerobic nitrate reduction by strain HCF1. Strain HCF1 is capable of reducing millimolar quantities of nitrate when growing with lactate (Figure 3A). However, under these conditions, nitrate reduction did not closely mirror lactate consumption; the most rapid lactate consumption occurred between 24 and 36 hr whereas the most rapid nitrate reduction occurred between 36 and 48 hr (Figure 3A). Beginning at 36 hr, nitrite began to accumulate and propionate and acetate

production began to deviate from that observed during growth without nitrate (specifically, acetate production was greater and propionate production lower in the presence of nitrate, despite similar lactate consumption rates in the presence and absence of nitrate). Since most nitrite accumulation occurred after lactate was depleted, it is not clear what electron donor was driving nitrate reduction after 48 hr. Possibilities include lactate-derived formate and H_2, although these two compounds should also have been present during lactate fermentation. Indeed, cell suspension studies in which H_2 was the only electron donor supplied (90% H_2/10% CO_2 in the headspace) resulted in nitrate reduction to nitrite, whereas controls with no electron donor supplied (80% N_2/20% CO_2 in the headspace) did not generate nitrite (Figure S4). For the study represented in Figure 3, it is likely that nitrite was reduced further to ammonium, based upon two observations: (a) the amount of accumulated nitrite accounted for only approximately half of the nitrate reduced and (b) an ammonium-forming nitrite reductase (*nrfA*; two copies) is encoded in the genome (see below). More insight on nitrate/nitrite reduction was provided by targeted transcriptional analysis (reverse transcription quantitative Polymerase Chain Reaction, or RT-qPCR) of three putative nitrate or nitrite reductase genes conducted for samples collected at 36 and 72 hr in the presence and absence of nitrate (Figure 3B); these data are addressed in the section on *c*-type cytochromes below.

Phylogeny of *Pelosinus* sp. strain HCF1. Based on its 16S rRNA gene sequence, strain HCF1 belongs to the *Pelosinus*-*Sporotalea* group in the Firmicutes (Figure 4). It is most closely related to *Pelosinus fermentans* R7 (27) and *Sporotalea propionicum* TmPN3 (28), whose 16S rRNA gene sequences share 98.0% and 95.0% identity, respectively, with that of strain HCF1. Notably, two distinct 16S rRNA gene copies of differing lengths were amplified from strain HCF1 using universal forward (27F) and reverse (1492R) primers. The longer 16S rRNA gene

of strain HCF1 contains an additional ~100-bp insertion region at the 5' end, whereas the rest of the two sequences are identical. Similarly, it has been reported that two length-variable copies of the 16S rRNA gene exist in *Pelosinus* sp. UFO1 and *Sporotalea* sp. TM1 (29), suggesting that this is not an unusual phenomenon in the *Pelosinus*-*Sporotalea* group (Figure 4). Whether or not the longer copy in the strain HCF1 genome is a pseudogene remains to be determined.

Overview of the *Pelosinus* sp. strain HCF1 genome. A draft sequence of the genome of *Pelosinus* sp. strain HCF1 was obtained by paired-end sequencing on an Illumina GAIIx platform. After quality control, the 100-bp paired-end reads were assembled into 214 contigs using Velvet (20) and coverage of 48x with an N50 of 79.5 Kb and maximum contig length of 288 Kb. The genome size is estimated at 4.98 Mb with a GC content of 39.8 % (Table 1).

Lactate fermentation by strain HCF1 proceeds via the methylmalonyl-CoA pathway. Analysis of the genome sequence of strain HCF1 indicates that it ferments lactate to propionate *via* the methylmalonyl-CoA pathway. The proposed enzymatic reactions involved in lactate fermentation by strain HCF1 are shown in Figure 5A. As proposed, lactate is converted to pyruvate by lactate dehydrogenase (multiple copies are present in the genome). Pyruvate can be converted to acetyl-CoA by pyruvate formate-lyase (PFL; two copies are present in the genome, Hcf1DRAFT_00614 and Hcf1DRAFT_04611, with adjacent genes encoding a PFL activase). In addition, pyruvate can be converted to acetyl-CoA by pyruvate:ferredoxin/flavodoxin oxidoreductase (PFOR; Hcf1DRAFT_02505), which can generate reduced ferredoxin as an electron donor for hydrogenases. Acetyl-CoA can be converted to acetate (with ATP generation from substrate-level phosphorylation) *via* phosphotransacetylase (Pta; Hcf1DRAFT_00266) and acetate kinase (Ack; Hcf1DRAFT_03144).

The pathway from pyruvate to propionate through methylmalonyl-CoA appears similar to that used by the close relative *Veillonella parvula* strain DSM 2008 (GenBank NC_013520); to illustrate, similar organization for selected genes in the methylmalonyl-CoA pathway in both organisms is shown in Figure 5B. However, strain HCF1 and *V. parvula* may differ in the enzymes catalyzing pyruvate carboxylation to oxaloacetate. For *V. parvula*, this is likely catalyzed by pyruvate carboxylase (Vpar_0752), but BLASTP searching (18) for this gene product did not result in any hits in the HCF1 genome. Instead, it is possible that pyruvate is converted to oxaloacetate by oxaloacetate decarboxylase [OAD; Hcf1DRAFT_02350 shares 50% sequence identity to the alpha subunit of OAD in *Vibrio cholera* (PDB accession number 2NX9)]. However, this same gene (Hcf1DRAFT_02350) was also tentatively annotated as pyruvate carboxylase subunit B and does not occur in a cluster with the beta and gamma subunits of OAD as does the alpha subunit of OAD in *Vibrio cholera*. Subsequent steps (Figure 5A) could be catalyzed by malate dehydrogenase (Hcf1DRAFT_00468), fumarase (e.g., Hcf1DRAFT_00270), and succinate dehydrogenase (Hcf1DRAFT_02750-2). Propionate formation is proposed to occur *via* propionyl-CoA:succinate CoA transferase [Hcf1DRAFT_02208; this shares 41% sequence identity with *E. coli* YgfH, which was demonstrated to have this activity (30)]. Other enzymes in the proposed pathway (Figure 5A) include methylmalonyl-CoA mutase (Hcf1DRAFT_00246-7 and Hcf1DRAFT_02209-10), methylmalonyl-CoA epimerase (Hcf1DRAFT_03696 and Hcf1DRAFT_03033, which share 97% sequence identity), and the Na^+ ion-translocating methylmalonyl-CoA decarboxylase (the alpha subunit is likely Hcf1DRAFT_03697, which shares 79% sequence identity with Vpar_1244 in *V. parvula*; the beta subunit is likely encoded by Hcf1DRAFT_03584, Hcf1DRAFT_04139, and Hcf1DRAFT_01795, which collectively share from 55 to 79%

sequence identity with Vpar_1240). Note that the last enzyme, methylmalonyl-CoA decarboxylase, is not used by a better-studied lactate-fermenting bacterium, *Propionibacterium freudenreichii*, which instead uses methylmalonyl-CoA carboxytransferase to simultaneously decarboxylate (*S*)-methylmalonyl-CoA to propionyl-CoA and carboxylate pyruvate to oxaloacetate (31, 32). Many of the genes cited in this section appear likely to have been mis-annotated by automated annotation pipelines. Our re-annotation of some of these genes was based in part on gene context. As shown in Figure 5B, a number of the genes putatively encoding the methylmalonyl-CoA pathway in *V. parvula* and strain HCF1 are organized in similar gene clusters. Experimental validation of the functions of some of these genes is required for more definitive annotation.

[FeFe]- and [NiFe]-hydrogenases in strain HCF1. The genome of fermentative strain HCF1 encodes an assortment of [NiFe]- and [FeFe]-hydrogenases, which are proposed to catalyze H_2 oxidation and H_2 production, respectively. The two [NiFe]-hydrogenases are likely membrane-associated respiratory uptake (H_2-oxidizing) hydrogenases [classified as Group 1 hydrogenases by Vignais and co-workers (33)]. The structural genes of the two [NiFe]-hydrogenases are localized in clusters that include genes for the three subunits (i.e., large, small, and *b*-type cytochrome). One [NiFe]-hydrogenase includes the genes Hcf1DRAFT_03506-03510 and the other includes Hcf1DRAFT_02596-02598 (with some "adjacent" genes on opposite DNA strands). Genes encoding proteins required for [NiFe]-hydrogenase assembly and maturation were identified, including *hypFCDE* (Hcf1DRAFT_00423-00420), *hypAB* (Hcf1DRAFT_00123-00122), and Hcf1DRAFT_03507-03506.

There is evidence for at least four [FeFe]-hydrogenases encoded in the genome of strain HCF1. Hcf1DRAFT_00661 was annotated as a ferredoxin hydrogenase large subunit, and

appears to belong to the Group B1 monomeric [FeFe]-hydrogenases [as described by Calusinska and co-workers (34)]. Hcf1DRAFT_02066 was also annotated as a ferredoxin hydrogenase large subunit but shares only 21% amino acid sequence identity with Hcf1DRAFT_00661. Hcf1DRAFT_02066 is part of a gene cluster that includes an alpha subunit of formate dehydrogenase (Hcf1DRAFT_02068), as has been observed for [FeFe]-hydrogenases identified in *Eubacterium acidaminophilum* and a variety of *Clostridia* spp. (34, 35). Considering the co-location of [Fe-Fe]-hydrogenase and formate dehydrogenase genes, it is possible that the formate dehydrogenase interacts with the hydrogenase in a complex linking formate oxidation to H^+ reduction.

Another putative [Fe-Fe]-hydrogenase is Hcf1DRAFT_01773, which occurs in a 3-gene cluster (Hcf1DRAFT_01771-01773). Considerable sequence similarity exists between these three genes and NuoEFG, which are subunits of Complex I (NADH:ubiquinone oxidoreductase); such similarity has been observed previously for certain [FeFe]-hydrogenases (33).

A fourth putative [Fe-Fe]-hydrogenase, Hcf1DRAFT_02349, appears to belong to the Group B2 monomeric [FeFe]-hydrogenases [as described by Calusinska and co-workers (34)]. Notably, an adjacent gene, Hcf1DRAFT_02350, is putatively pyruvate carboxylase or oxaloacetate decarboxylase, which is involved in lactate fermentation to propionate (as discussed earlier).

Transcriptional studies of strain HCF1 were undertaken to explore differential expression of structural genes representing the two [NiFe]-hydrogenases and four [FeFe]-hydrogenases under several anaerobic conditions: (a) H_2 (a 90% H_2/10 CO_2 mixture) as the sole electron donor, (b) lactate with no H_2 (80% N_2/20% CO_2 headspace), and (c) fructose with no H_2 (80% N_2/20% CO_2 headspace). Although definitive trends were not apparent to distinguish expression among

three conditions tested, one clear trend was that one [NiFe]-hydrogenase (represented by HCF1DRAFT_03510) was expressed at significantly higher levels than the other five hydrogenases tested (on average, ~8-fold higher, normalized to *rpoB* and averaged across all conditions examined) (Table S3).

Putative chromate reductases and *c*-type cytochromes in strain HCF1. Although many chromate-reducing bacterial species have been reported, only for a relatively small subset of these bacteria have the proteins catalyzing Cr(VI) reduction been identified and characterized biochemically, as reviewed elsewhere (36, 37). To date, the best-studied chromate reductase is ChrR, a soluble, dimeric, NADH-dependent flavoprotein reported in *Pseudomonas putida* (38, 39). BLASTP searches of the strain HCF1 genome were conducted for the following chromate reductases: ChrR from *P. putida* (GenBank AF375642); an Old Yellow Enzyme (OYE) homolog from *Thermus scotoductis* [(40); GenBank AM902709]; YieF, a ChrR homlog from *E. coli* [(38); GenBank AAK62985.2]; the Fre flavin reductase from *E. coli* [(25); EcoCyc EG10334]; FerB from *Paracoccus denitrificans* [(41, 42); putatively GenBank YP_917833.1]; and an azoreductase from *Bacillus* sp OY1-2 [(43); GenBank BAB13746.1]. The best match to any of these proteins was Hcf1DRAFT_04683, whose predicted protein sequence shared 51% identity with ChrR from *P. putida*. Alignment of these two proteins (Figure S5) revealed high conservation of the LFVTPEYNXXXXXXLKNAIDXXS motif in Hcf1DRAFT_04683 (with a leucine-to-isoleucine deviation at position 90), indicating that it is a member of the NADH_dh2 family of putative flavin-binding quinone reductases (39). Notably, Hcf1DRAFT_04683 also shared 42% sequence identity with the FerB flavoprotein, which has been shown to be effective at reducing Fe(III)-NTA as well as Cr(VI) (41, 42) and thus could be relevant to Fe(III) reduction in strain HCF1. The only other BLASTP match of note was Hcf1DRAFT_00464,

which shared 45% protein sequence identity with the NAD(P)H:flavin oxidoreductase (OYE homolog) from *T. scotoductis*.

Motivated in part by a desire to identify candidate *c*-type cytochromes that might be catalyzing Fe(III) or Cr(VI) reduction in strain HCF1, we searched all strain HCF1 ORFs for the CXXCH heme-binding motif that characterizes *c*-type cytochromes. Of the 37 ORFs found to contain one or more instances of the CXXCH motif, most were clearly not *c*-type cytochromes (including many Fe-S proteins, the molecular chaperone DnaJ, and ribosomal proteins L31 and L32, among others). A list of encoded proteins containing a CXXCH motif is shown in Table 2; all genes with annotations clearly indicating that they do not encode *c*-type cytochromes have been excluded from the table, leaving only 13 genes, most of which are annotated as "hypothetical proteins". There was no evidence of the multi-heme *c*-type cytochromes that have been reported to catalyze Fe(III) reduction in *Geobacter* and *Shewanella* species (44). Instead, the five encoded *c*-type cytochromes that could be confidently annotated are all related to the reduction of nitrogen oxides (nitrate, nitrite, or nitric oxide). Included in the HCF1 genome are two highly similar (sharing 58 to 68% amino acid sequence identity) pairs of *c*-type cytochrome genes encoding a nitrite reductase complex composed of NrfH and NrfA (formate-dependent nitrite reductase): Hcf1DRAFT_02324-02323 and Hcf1DRAFT_00451-00450. In both cases, these genes are clustered with upstream cytochrome *c* biosynthesis genes. The NrfHA nitrite reductase complex could play a key role in the dissimilatory reduction of nitrate to ammonium coupled to the oxidation of formate or H_2, as has been reported in certain proteobacteria, such as *Wolinella succinogenes* (45). Notably, the genome of strain HCF1 also encodes a membrane-bound, respiratory nitrate reductase (*narGHJI*; Hcf1DRAFT_02301-02298), which could reduce nitrate to nitrite, thereby supplying nitrite to the NrfHA nitrite reductase complex. Thus, it is

possible that formate- or H_2-dependent dissimilatory reduction of nitrate to ammonium catalyzed by NarG, NrfA, and NrfH (among other proteins) is responsible for the previously discussed observation of nitrate reduction occurring during growth of strain HCF1 with lactate (Figure 3A). Transcriptional (RT-qPCR) analyses of *narG* and the two putative *nrfH* copies in cultures of strain HCF1 growing with lactate in the presence and absence of nitrate provide some insight on which nitrate and nitrite reductases may be involved. It is clear (Figure 3B) that both *narG* (Hcf1DRAFT_02301) and "*nrfH2*" (Hcf1DRAFT_02324) are nitrate-inducible, whereas "*nrfH1*" (Hcf1DRAFT_00451) is apparently not and is less likely to be catalyzing nitrite reduction under the conditions tested.

Finally, to complete the list of well-defined *c*-type cytochromes encoded in the HCF1 genome, we identified a membrane-anchored nitric oxide reductase, which includes the *c*-type cytochrome NorC (Hcf1DRAFT_04668) and the *b*-type cytochrome NorB (Hcf1DRAFT_04669). The presence of nitric oxide reductase in strain HCF1 is unexpected, as this enzyme is typically associated with denitrification, and the genome sequence does not indicate that strain HCF1 has this capability (i.e., we could not identify genes encoding nitric oxide-forming nitrite reductases, such as NirS or NirK, or the nitrous oxide reductase, NosZ). BLASTp searches of the closely related fermenter *V. parvula* and a range of *Clostridium* species did not reveal any matches to the NorC of strain HCF1.

Dominance of *Pelosinus* sp. strain HCF1 in laboratory systems inoculated with aquifer material from the Hanford 100H site. Analysis by PCR amplification and pyrosequencing of SSU rRNA genes from fermenting column effluents demonstrated that a 16S rRNA gene taxon, identical to strain HCF1 over the region amplified (V4-V5 hypervariable region), was the dominant taxon, representing almost 80% of the pyrotag reads (Figure 6).

Environmental relevance of *Pelosinus* sp. strain HCF1. *Pelosinus* sp. strain HCF1 and close relatives have been reported as dominant microbial community members in experimental systems inoculated with Hanford 100H aquifer sediment (Figure 6) and groundwater (2) as well as laboratory (46) and field (5) aquifer systems associated with the Integrated Field Research Challenge site located at Oak Ridge National Laboratory (Tennessee). Considering its ability to become a prominent member of aquifer microbial communities and its diverse metabolic capabilities, *Pelosinus* sp. strain HCF1 (and close relatives) could play an important role in multiple biogeochemical cycles in aquifer environments. For example, in addition to catalyzing *in situ* Cr(VI) reduction under fermentative conditions in contaminated aquifers, it could potentially also reduce U(VI) (2, 47), nitrate (to nitrite and ammonium), and Fe(III). Although these reductive processes may not all be coupled to energy conservation in strain HCF1, they nonetheless could directly or indirectly mediate the mobility, toxicity, and bioavailability of several elements of environmental relevance. Strain HCF1 can also ferment a range of substrates relevant to both native and engineered conditions and could thereby release important metabolites for interspecies transfer, including acetate, propionate, H_2, and formate. Overall, the metabolic activities of strain HCF1 could mediate biogeochemical processes affecting the physicochemical and microbial components of its local aquifer environment.

Genomic and focused transcriptional analyses of strain HCF1 reported here have provided some insights into the underlying genetic basis of some of this organism's metabolic capabilities, including the methylmalonyl-CoA pathway and associated enzymes that catalyze the fermentation of lactate (and other substrates) to propionate and acetate, a variety of [NiFe]- and [FeFe]-hydrogenases that likely catalyze both H_2 production and consumption, flavoproteins that may catalyze Cr(VI) and Fe(III) reduction, and nitrate and nitrite reductases (NrfH, NrfA,

and NarGHI) that likely play a role in dissimilatory reduction of nitrate to ammonium. These nitrite reductases (*nrfH* and *nrfA*), along with nitric oxide reductase (*norCB*), are among the unexpected genes identified in the genome of strain HCF1 (e.g., BLASTP searches revealed no homologs in the *V. parvula* genome). To date, identification of *nrfA* in any firmicute genome is rare (as indicated by the FunGene database; http://fungene.cme.msu.edu; 6/7/2012 release). The metabolic context relevant to some of the genes identified in strain HCF1, such as nitric oxide reductase, is not currently understood. Understanding should improve as a result of future studies that will focus on characterizing the gene expression of strain HCF1 in an environmentally relevant context, such as in flow-through columns constructed with Hanford 100H aquifer sediment and eluted with synthetic groundwater that simulates *in situ* conditions.

ACKNOWLEDGMENTS

This work was supported as part of the Subsurface Biogeochemical Research Scientific Focus Area funded by the U.S. Department of Energy, Office of Science, Office of Biological and Environmental Research under Award Number DE-AC02-05CH11231. We thank Joern Larsen, Li Yang, and Jasselle Cabugao (LBNL) for valuable technical assistance.

REFERENCES

1. **Brodie EL, Joyner DC, Faybishenko B, Conrad ME, Rios-Velazquez C, Malave J, Martinez R, Mork B, Willett A, Koenigsberg S, Herman DJ, Firestone MK, Hazen TC.** 2011. Microbial community response to addition of polylactate compounds to stimulate hexavalent chromium reduction in groundwater. Chemosphere **85:**660-665.
2. **Mosher JJ, Phelps TJ, Podar M, Hurt RA, Jr., Campbell JH, Drake MM, Moberly JG, Schadt CW, Brown SD, Hazen TC, Arkin AP, Palumbo AV, Faybishenko BA, Elias**

DA. 2012. Microbial community succession during lactate amendment and electron acceptor limitation reveals a predominance of metal-reducing *Pelosinus* spp. Appl. Environ. Microbiol. **78:**2082-2091.

3. **Moe WM, Stebbing RE, Rao JU, Bowman KS, Nobre MF, da Costa MS, Rainey FA.** 2012. *Pelosinus defluvii* sp. nov., isolated from chlorinated solvent-contaminated groundwater, emended description of the genus *Pelosinus* and transfer of *Sporotalea propionica* to *Pelosinus propionicus* comb. nov. Int. J. Syst. Evol. Microbiol. **62:**1369-1376.
4. **Gihring TM, Zhang G, Brandt CC, Brooks SC, Campbell JH, Carroll S, Criddle CS, Green SJ, Jardine P, Kostka JE, Lowe K, Mehlhorn TL, Overholt W, Watson DB, Yang Z, Wu WM, Schadt CW.** 2011. A limited microbial consortium is responsible for extended bioreduction of uranium in a contaminated aquifer. Appl. Environ. Microbiol. **77:**5955-5965.
5. **Schadt C, Gihring T, Carroll S, Mehlhorn T, Yang Z, Kerley M, Elias D, Watson D, Brooks S, Doktycz C, Merryfield J, Kostka J**. New isolates of *Geobacter*, *Desulforegula*, *Desulfovibrio*, and *Pelosinus* and their roles in a low diversity consortia during sustained *in situ* reduction of U(VI). In *Abstracts of Subusrface Biogoechemical Research Annual Meeting, April 30 - May 2, 2012*, US Department of Energy: Washington, DC, 2012.
6. **Costa M, Klein CB.** 2006. Toxicity and carcinogenicity of chromium compounds in humans. Critical Reviews in Toxicology **36:**155-163.
7. **Cieslak-Golonka M.** 1996. Toxic and mutagenic effects of chromium(VI). A review. Polyhedron **15:**3667-3689.
8. **Hungate R, Macy J.** 1973. The roll-tube technique for cultivation of strict anaerobes. Bull. Ecol. Res. Comm. (Stockholm) **17:**123-125.

9. **Han R, Geller JT, Yang L, Brodie EL, Chakraborty R, Larsen JT, Beller HR.** 2010. Physiological and transcriptional studies of Cr(VI) reduction under aerobic and denitrifying conditions by an aquifer-derived pseudomonad. Environ. Sci. Technol. **44:**7491-7497.
10. **Beller H, Spormann A, Sharma P, Cole J, Reinhard M.** 1996. Isolation and characterization of a novel toluene-degrading, sulfate- reducing bacterium. Appl. Environ. Microbiol. **62:**1188-1196.
11. **Beller HR, Grbic-Galic D, Reinhard M.** 1992. Microbial degradation of toluene under sulfate-reducing conditions and the influence of iron on the process. Appl. Environ. Microbiol. **58:**786-793.
12. **Stookey L.** 1970. Ferrozine - a new spectrophotometric reagent for iron. Analytical Chemistry **42:**779-781.
13. **Ivanov, II, Atarashi K, Manel N, Brodie EL, Shima T, Karaoz U, Wei D, Goldfarb KC, Santee CA, Lynch SV, Tanoue T, Imaoka A, Itoh K, Takeda K, Umesaki Y, Honda K, Littman DR.** 2009. Induction of intestinal Th17 cells by segmented filamentous bacteria. Cell **139:**485-498.
14. **Hamady M, Walker JJ, Harris JK, Gold NJ, Knight R.** 2008. Error-correcting barcoded primers for pyrosequencing hundreds of samples in multiplex. Nature Methods **5:**235-237.
15. **Caporaso JG, Kuczynski J, Stombaugh J, Bittinger K, Bushman FD, Costello EK, Fierer N, Pena AG, Goodrich JK, Gordon JI et al.** 2010. QIIME allows analysis of high-throughput community sequencing data. Nature Methods **7:**335-336.
16. **Wang Q, Garrity GM, Tiedje JM, Cole JR.** 2007. Naive Bayesian classifier for rapid assignment of rRNA sequences into the new bacterial taxonomy. Appl. Environ. Microbiol. **73:**5261-5267.

17. **Lane D.** 16S/23S rRNA sequencing. *In* Nucleic Acid Techniques in Bacterial Systematics, Stackebrandt E, Goodfellow M, Eds. John Wiley & Sons: Chichester, UK, 1991; pp 115-175.

18. **Altschul SF, Madden TL, Schaffer AA, Zhang J, Zhang Z, Miller W, Lipman DJ.** 1997. Gapped BLAST and PSI-BLAST: a new generation of protein database search programs. Nucleic Acids Res. **25:**3389-3402.

19. **Tamura K, Dudley J, Nei M, Kumar S.** 2007. MEGA4: Molecular Evolutionary Genetics Analysis (MEGA) software version 4.0. Mol Biol Evol **24:**1596-1599.

20. **Zerbino DR, Birney E.** 2008. Velvet: Algorithms for *de novo* short read assembly using de Bruijn graphs. Genome Res. **18:**821-829.

21. **Markowitz VM, Chen IMA, Palaniappan K, Chu K, Szeto E, Grechkin Y, Ratner A, Jacob B, Huang J, Williams P.** 2012. IMG: the integrated microbial genomes database and comparative analysis system. Nucleic Acids Res. **40:**D115-D122.

22. **Rozen S, Skaletsky H.** Primer3 on the WWW for General Users and for Biologist Programmers. In Bioinformatics Methods and Protocols, 1999; pp 365-386.

23. **Faybishenko B, Hazen TC, Long PE, Brodie EL, Conrad ME, Hubbard SS, Christensen JN, Joyner D, Borglin SE, Chakraborty R, Williams KH, Peterson JE, Chen J, Brown ST, Tokunaga TK, Wan J, Firestone M, Newcomer DR, Resch CT, Cantrell KJ, Willett A, Koenigsberg S.** 2008. *In situ* long-term reductive bioimmobilization of Cr(VI) in groundwater using Hydrogen Release Compound. Environ. Sci. Technol. **42:**8478-8485.

24. **Rai D, Sass BM, Moore DA.** 1987. Chromium(III) hydrolysis constants and solubility of chromium(III) hydroxide. Inorganic Chemistry **26:**345-349.

25. **Puzon GJ, Petersen JN, Roberts AG, Kramer DM, Xun L.** 2002. A bacterial flavin reductase system reduces chromate to a soluble chromium(III)-NAD^+ complex. Biochem. Biophys. Res. Commun. **294:**76-81.

26. **Puzon GJ, Roberts AG, Kramer DM, Xun L.** 2005. Formation of soluble organo-chromium(III) complexes after chromate reduction in the presence of cellular organics. Environ. Sci. Technol. **39:**2811-2817.

27. **Shelobolina ES, Nevin KP, Blakeney-Hayward JD, Johnsen CV, Plaia TW, Krader P, Woodard T, Holmes DE, Vanpraagh CG, Lovley DR.** 2007. *Geobacter pickeringii* sp. nov., *Geobacter argillaceus* sp. nov. and *Pelosinus fermentans* gen. nov., sp. nov., isolated from subsurface kaolin lenses. Int. J. Syst. Evol. Microbiol. **57:**126-135.

28. **Boga HI, Ji R, Ludwig W, Brune A.** 2007. *Sporotalea propionica* gen. nov. sp. nov., a hydrogen-oxidizing, oxygen-reducing, propionigenic firmicute from the intestinal tract of a soil-feeding termite. Archives of Microbiology **187:**15-27.

29. **Ray AE, Connon SA, Sheridan PP, Gilbreath J, Shields M, Newby DT, Fujita Y, Magnuson TS.** 2010. Intragenomic heterogeneity of the 16S rRNA gene in strain UFO1 caused by a 100-bp insertion in helix 6. FEMS Microbiology Ecology **72:**343-353.

30. **Haller T, Buckel T, Retey J, Gerlt JA.** 2000. Discovering new enzymes and metabolic pathways: conversion of succinate to propionate by *Escherichia coli*. Biochemistry **39:**4622-4629.

31. **Hoffmann A, Hilpert W, Dimroth P.** 1989. The carboxyltransferase activity of the sodium-ion-translocating methylmalonyl-CoA decarboxylase of *Veillonella alcalescens*. Eur. J. Biochem. **179:**645-650.

32. **Seeliger S, Janssen PH, Schink B.** 2002. Energetics and kinetics of lactate fermentation to acetate and propionate via methylmalonyl-CoA or acrylyl-CoA. FEMS Microbiol. Lett. **211:**65-70.

33. **Vignais PM, Billoud B, Meyer J.** 2001. Classification and phylogeny of hydrogenases. FEMS Microbiol. Rev. **25:**455-501.

34. **Calusinska M, Happe T, Joris B, Wilmotte A.** 2010. The surprising diversity of clostridial hydrogenases: a comparative genomic perspective. Microbiology **156:**1575-1588.

35. **Graentzdoerffer A, Rauh D, Pich A, Andreesen JR.** 2003. Molecular and biochemical characterization of two tungsten- and selenium-containing formate dehydrogenases from *Eubacterium acidaminophilum* that are associated with components of an iron-only hydrogenase. Archives of Microbiology **179:**116-130.

36. **Cheung K, Gu J-D.** 2007. Mechanism of hexavalent chromium detoxification by microorganisms and bioremediation application potential: A review. International Biodeterioration & Biodegradation **59:**8-15.

37. **Ramirez-Diaz MI, Diaz-Perez C, Vargas E, Riveros-Rosas H, Campos-Garcia J, Cervantes C.** 2008. Mechanisms of bacterial resistance to chromium compounds. Biometals **21:**321-332.

38. **Ackerley DF, Gonzalez CF, Park CH, Blake R, 2nd, Keyhan M, Matin A.** 2004. Chromate-reducing properties of soluble flavoproteins from *Pseudomonas putida* and *Escherichia coli*. Appl. Environ. Microbiol. **70:**873-882.

39. **Gonzalez CF, Ackerley DF, Lynch SV, Matin A.** 2005. ChrR, a soluble quinone reductase of *Pseudomonas putida* that defends against H_2O_2. J. Biol. Chem. **280:**22590-22595.

40. **Opperman DJ, Piater LA, van Heerden E.** 2008. A novel chromate reductase from *Thermus scotoductus* SA-01 related to old yellow enzyme. J. Bacteriol. **190:**3076-3082.
41. **Mazoch J, Tesarik R, Sedlacek V, Kucera I, Turanek J.** 2004. Isolation and biochemical characterization of two soluble iron(III) reductases from *Paracoccus denitrificans*. Eur. J. Biochem. **271:**553-562.
42. **Sedlacek V, Kucera I.** 2010. Chromate reductase activity of the *Paracoccus denitrificans* ferric reductase B (FerB) protein and its physiological relevance. Archives of Microbiology **192:**919-926.
43. **Suzuki Y, Yoda T, Ruhul A, Sugiura W.** 2001. Molecular cloning and characterization of the gene coding for azoreductase from *Bacillus* sp. OY1-2 isolated from soil. J. Biol. Chem. **276:**9059-9065.
44. **Weber KA, Achenbach LA, Coates JD.** 2006. Microorganisms pumping iron: anaerobic microbial iron oxidation and reduction. Nat. Rev. Microbiol. **4:**752-764.
45. **Simon J.** 2002. Enzymology and bioenergetics of respiratory nitrite ammonification. FEMS Microbiol. Rev. **26:**285-309.
46. **Yang F, Tiedje JM, Zhou J, Marsh T.** Firmicutes and their roles in uranium immobilization. In *Abstracts of Subusrface Biogoechemical Research Annual Meeting, April 30 - May 2, 2012*, US Department of Energy: Washington, DC, 2012.
47. **Ray A, Bargar J, Sivaswamy V, Dohnalkova A, Fujita Y, Peyton B, Magnuson T.** 2010. Evidence for multiple modes of uranium immobilization by an anaerobic bacterium. Geochim. Cosmochim. Acta **75:**2684-2695.

FIGURE LEGENDS

FIGURE 1. Results of cell suspension assays to determine reduction of Cr(VI) by strain HCF1 under fermentative conditions with lactate (20 mM) as the electron donor. (A) Dissolved Cr(VI) concentrations as determined by the DPC assay. (B) Dissolved total Cr concentrations as determined by ICP-MS in aliquots of the same samples represented in panel A. Cell densities were approximately 2.2 x 10^9 cells/mL. Note that the slightly lower time-zero concentrations for lactate-containing samples in panel A compared to panel B are likely due to a minor effect of lactate on the DPC assay (9).

FIGURE 2. Results of cell suspension assays to determine reduction of Fe(III)-NTA by strain HCF1 under fermentative conditions with lactate (20 mM) as the electron donor. Data points represent averages of duplicates and error bars represent 1 standard deviation. Cell densities were approximately 1.3 x 10^9 cells/mL.

FIGURE 3. Lactate fermentation under anaerobic growth conditions in the presence and absence of nitrate. (A) Concentrations of lactate, acetate, and propionate (left-hand axis) and nitrate and nitrite (right-hand axis); nitrate and nitrite are shown only for nitrate-amended replicates. Data points represent averages of duplicates and error bars represent 1 standard deviation. Black arrows indicate the sampling times for transcriptional analysis. (B) Transcript copy number (normalized to *rpoB*) determined by RT-qPCR for three genes: *narG* (Hcf1DRAFT_02301), *nrfH* - copy 1 (Hcf1DRAFT_00451), *nrfH* - copy 2 (Hcf1DRAFT_02324) in biological duplicates with and without nitrate (represented in panel A). Bar heights represent averages (n = 5 or 6, including technical replicates). Relative standard deviations averaged 24% and ranged from 13 to 46% (Table S4).

FIGURE 4. Maximum-likelihood phylogenetic tree of *Pelosinus* sp. strain HCF1 and representative Firmicutes. The bar represents distances calculated as described in Materials and Methods. Numbers at internal nodes are the percentage of 100 bootstrap samples in which the organisms to the right of the node were monophyletic.

FIGURE 5. (A) Proposed pathway for lactate fermentation to acetate and propionate in *Pelosinus* sp. strain HCF1 based on genomic analysis (see text). Abbreviations: Pta, phosphotransacetylase; Ack, acetate kinase; PFL, pyruvate formate-lyase; PFOR, pyruvate:ferredoxin/flavodoxin oxidoreductase; DH, dehydrogenase; CoA, coenzyme A. (B) Genomic organization of selected genes putatively involved in the methylmalonyl-CoA pathway in strain HCF1 and *Veillonella parvula*. Note that PCR finishing was used to establish that Hcf1DRAFT_2210 and Hcf1DRAFT_3695 are contiguous in the genome.

FIGURE 6. Phylogenetic composition of flow-through column microbial community from which strain HCF1 was isolated, based upon SSU rRNA gene pyrotag sequence analysis.

TABLE 1. *Pelosinus* sp. strain HCF1 sequencing and draft genome statistics

Platform	Illumina HiSeq 2000
Estimated genome size	4.98 Mb
Coverage	48X
Number of contigs	214
N50	79.5 kb
Largest contig	288 kb
G+C percentage	39.81%

	Count	**Percentage**
Genes, total number	4845	100.00%
Protein coding genes	4726	97.54%
RNA genes	119	2.46%
Protein coding genes with function prediction	3776	77.94%
CRISPR Count	2	

TABLE 2. CDS potentially encoding *c*-type cytochromes in the *Pelosinus* strain HCF1 genome[a]

Locus Tag	Annotation[b]	Molecular Mass (kDa)[c]	Number of Hemes
Hcf1DRAFT_00116	Hypothetical protein	15.1	1
Hcf1DRAFT_00157	Uncharacterized conserved protein	41.8	1
Hcf1DRAFT_00450	Formate-dependent nitrite reductase, periplasmic cytochrome c_{552} subunit (EC:1.7.2.2), NrfA	48.0	5
Hcf1DRAFT_00451	NrfH, a membrane-bound tetraheme cytochrome *c* subunit of the NapC/NirT family that interacts with NrfA	17.3	4
Hcf1DRAFT_00707	Hypothetical protein	16.5	1
Hcf1DRAFT_02259	Hypothetical protein	6.8	1
Hcf1DRAFT_02323	Formate-dependent nitrite reductase, periplasmic cytochrome c_{552} subunit (EC:1.7.2.2), NrfA	47.5	5
Hcf1DRAFT_02324	NrfH, a membrane-bound tetraheme cytochrome *c* subunit of the NapC/NirT family that interacts with NrfA	17.0	4
Hcf1DRAFT_02925	Hypothetical protein	22.5	1
Hcf1DRAFT_03482	Hypothetical protein	6.5	1
Hcf1DRAFT_03609	Hypothetical protein	8.3	1

Hcf1DRAFT_03838	Hypothetical protein	9.2	1
Hcf1DRAFT_04668	Putative nitric oxide reductase, NorC	15.8	1

a As defined by the presence of at least one CXXCH heme-binding motif but excluding proteins that are clearly not *c*-type cytochromes (see text). For NrfA, one additional heme is represented by a CXXCK motif (45).

b Best attempt at annotation based on examination of best BLASTP hits and genomic context.

c Molecular mass predicted for the unprocessed gene product without cofactors.

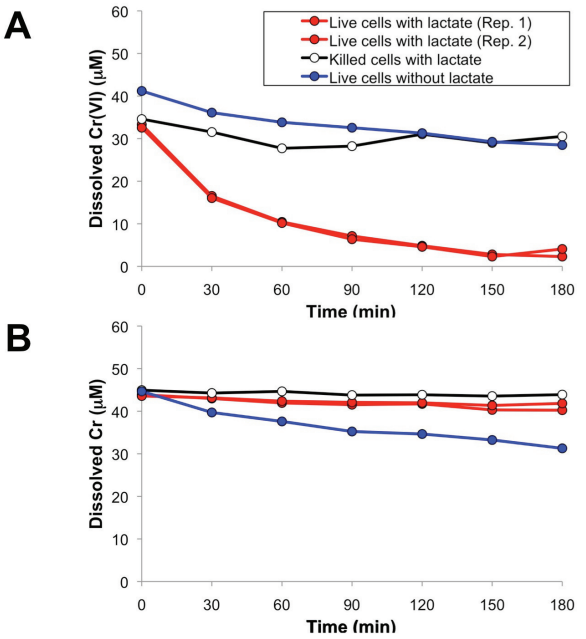
A
Live cells with lactate (Rep. 1)
Live cells with lactate (Rep. 2)
Killed cells with lactate
Live cells without lactate
Dissolved Cr(VI) (µM)
Time (min)
B
Dissolved Cr (µM)
Time (min)

Figure 1

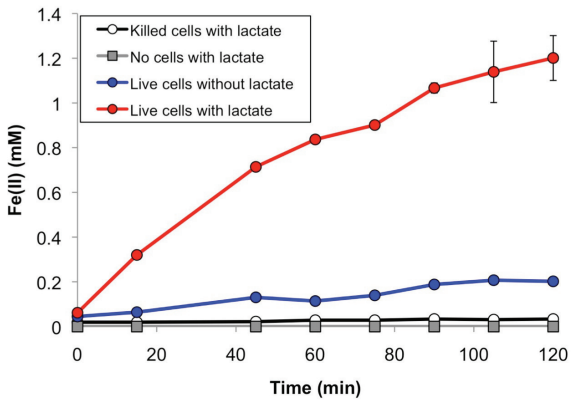
Killed cells with lactate
No cells with lactate
Live cells without lactate
Live cells with lactate
Fe(II) (mM)
Time (min)
0
0.2
0.4
0.6
0.8
1
1.2
1.4
0
20
40
60
80
100
120

Figure 2

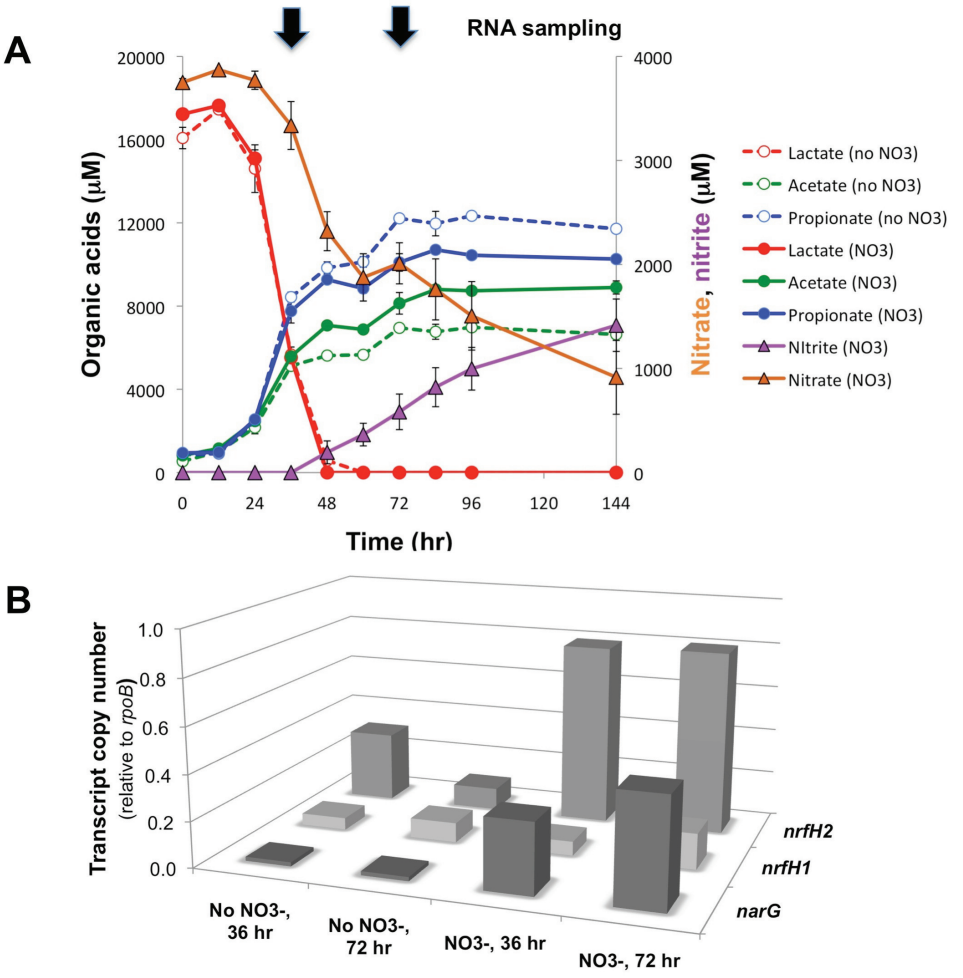
A
RNA sampling
Organic acids (μM)
Nitrate, nitrite (μM)
Time (hr)
Lactate (no NO3)
Acetate (no NO3)
Propionate (no NO3)
Lactate (NO3)
Acetate (NO3)
Propionate (NO3)
NItrite (NO3)
Nitrate (NO3)
B
Transcript copy number
(relative to rpoB)
nrfH2
nrfH1
narG
No NO3-, 36 hr
No NO3-, 72 hr
NO3-, 36 hr
NO3-, 72 hr

Figure 3

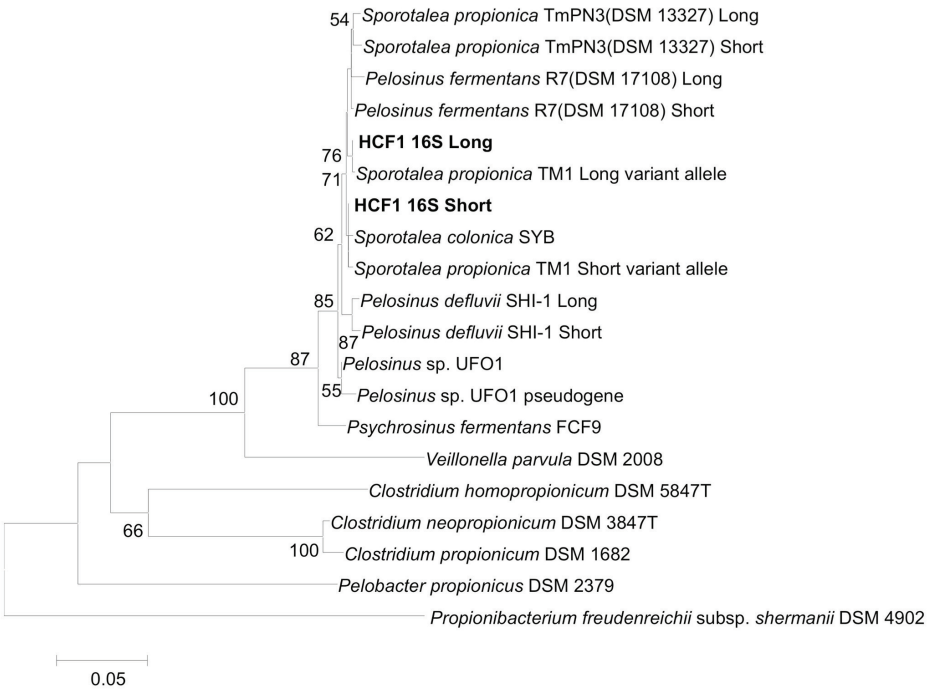
54
Sporotalea propionica TmPN3(DSM 13327) Long
Sporotalea propionica TmPN3(DSM 13327) Short
Pelosinus fermentans R7(DSM 17108) Long
Pelosinus fermentans R7(DSM 17108) Short
HCF1 16S Long
76
71
Sporotalea propionica TM1 Long variant allele
HCF1 16S Short
62
Sporotalea colonica SYB
Sporotalea propionica TM1 Short variant allele
85
Pelosinus defluvii SHI-1 Long
87
Pelosinus defluvii SHI-1 Short
87
Pelosinus sp. UFO1
55
Pelosinus sp. UFO1 pseudogene
100
Psychrosinus fermentans FCF9
Veillonella parvula DSM 2008
Clostridium homopropionicum DSM 5847T
66
Clostridium neopropionicum DSM 3847T
100
Clostridium propionicum DSM 1682
Pelobacter propionicus DSM 2379
Propionibacterium freudenreichii subsp. shermanii DSM 4902
0.05

Figure 4

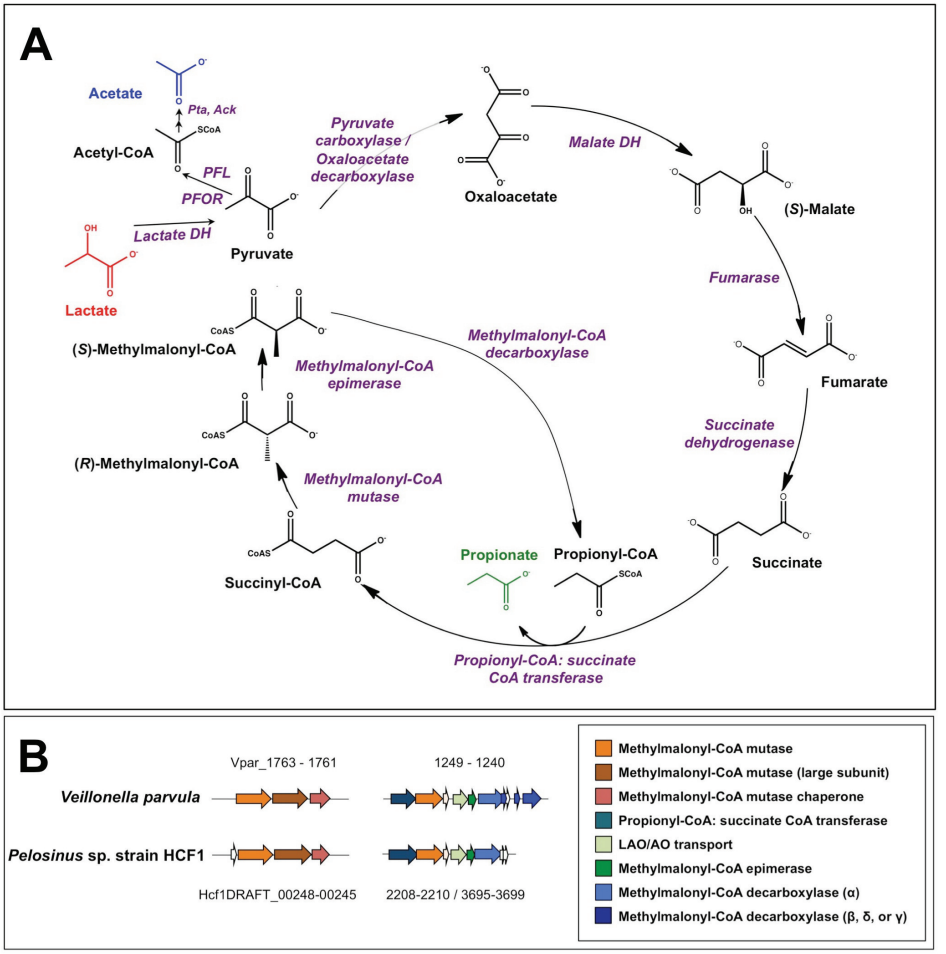
A
Acetate
Pta, Ack
Acetyl-CoA
SCoA
PFL
PFOR
Lactate DH
Pyruvate
Lactate
Pyruvate carboxylase / Oxaloacetate decarboxylase
Oxaloacetate
Malate DH
(S)-Malate
Fumarase
Fumarate
Succinate dehydrogenase
Succinate
(S)-Methylmalonyl-CoA
Methylmalonyl-CoA decarboxylase
Methylmalonyl-CoA epimerase
(R)-Methylmalonyl-CoA
Methylmalonyl-CoA mutase
Succinyl-CoA
Propionate
Propionyl-CoA
Propionyl-CoA: succinate CoA transferase
B
Vpar_1763 - 1761
1249 - 1240
Veillonella parvula
Pelosinus sp. strain HCF1
Hcf1DRAFT_00248-00245
2208-2210 / 3695-3699
Methylmalonyl-CoA mutase
Methylmalonyl-CoA mutase (large subunit)
Methylmalonyl-CoA mutase chaperone
Propionyl-CoA: succinate CoA transferase
LAO/AO transport
Methylmalonyl-CoA epimerase
Methylmalonyl-CoA decarboxylase (α)
Methylmalonyl-CoA decarboxylase (β, δ, or γ)

Figure 5

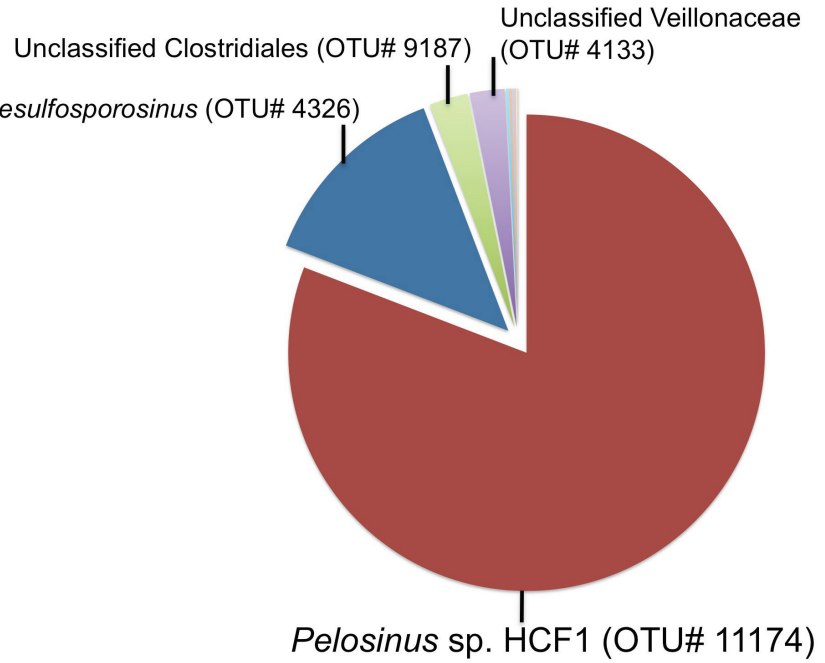
Unclassified Veillonaceae
(OTU# 4133)
Unclassified Clostridiales (OTU# 9187)
esulfosporosinus (OTU# 4326)
Pelosinus sp. HCF1 (OTU# 11174)

Figure 6

DISCLAIMER